Electronic Supplementary Information

A dynamically stable self-assembled CoFe (oxy)hydroxide-based nancatalyst with boosted electrocatalytic performance for oxygen-evolution reaction

Ming Zhu[a,b,1], Hengyue Xu[c,1], Jie Dai[d], Daqin Guan[c]*, Zhiwei Hu[e], Sixuan She[f], Chien-Te Chen[g], Ran Ran[a]*, Wei Zhou[a], and Zongping Shao[c]*

[a] State Key Laboratory of Materials-Oriented Chemical Engineering, College of Chemical Engineering, Nanjing Tech University, Nanjing, 211800, China

[b] Institute for Smart City of Chongqing University in Liyang, Chongqing University, Jiangsu, 213300, China

[c] WA School of Mines: Minerals, Energy and Chemical Engineering, Curtin University, Perth, Western Australia 6845, Australia

[d] School of Environmental Science and Engineering, Shanghai Jiao Tong University, Shanghai, 200240, China

[e] Max-Planck-Institute for Chemical Physics of Solids, Nöthnitzer Str. 40, Dresden 01187, Germany.

[f] Department of Applied Physics and Materials Research Center, The Hong Kong Polytechnic University, Hung Hom, Kowloon, Hong Kong

[g] National Synchrotron Radiation Research Center, 101 Hsin-Ann Road, Hsinchu 30076, Taiwan.

*Email: daqin.guan@curtin.edu.au, ranr@njtech.edu.cn, zongping.shao@curtin.edu.au

[1] These authors contributed equally: Ming Zhu, Hengyue Xu

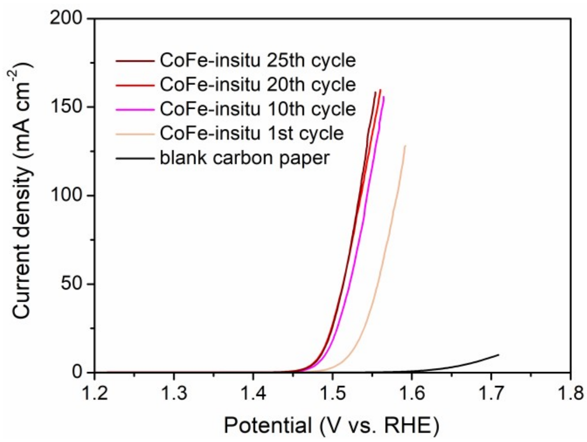

Figure S1. The LSV curves of CoFe-insitu during eletrpdeposition in 1M KOH.

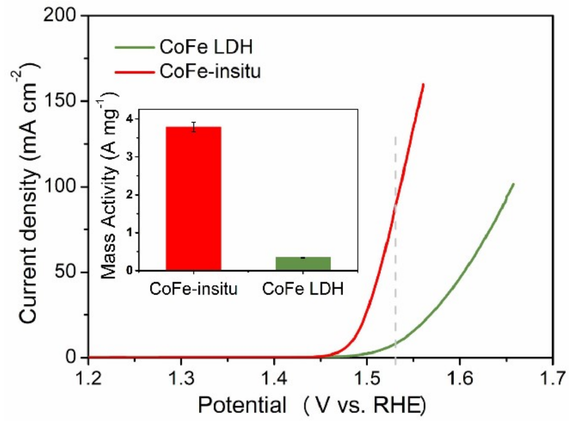

Figure S2. The OER polarization curves and mass activities of CoFe-insitu and CoFe LDH with the same mass loading (0.0146 mg cm^{-2} metal on the electrode) at η =0.3 V.

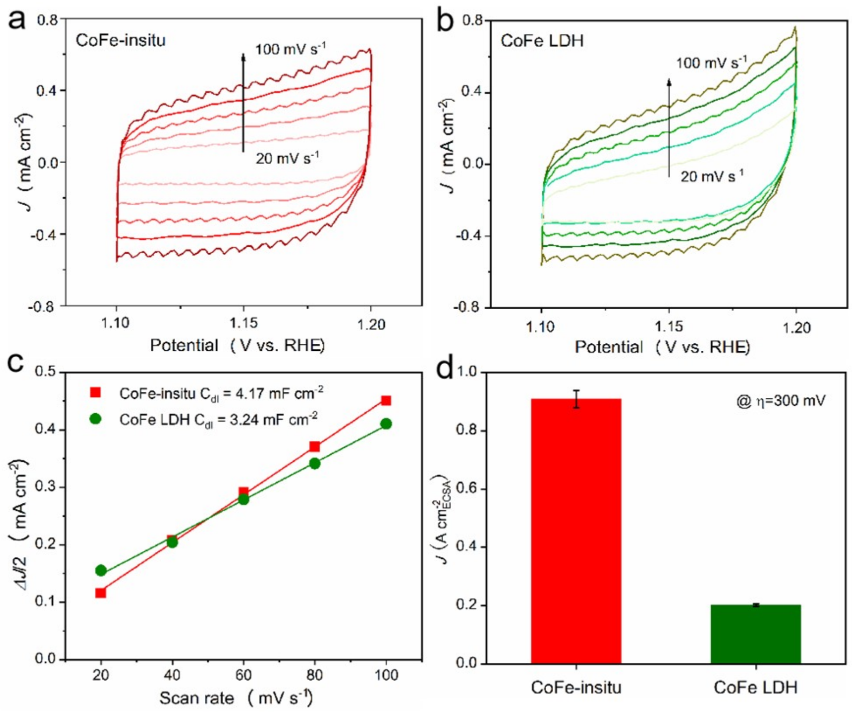

Figure S3. CV measurements in a non-faradic current region at scan rates of 20, 40, 60, 80 and 100 mV s^{-1} of a) CoFe-insitu, b) CoFe LDH. c)Linear fitting of the capacitive currents versus CV scan rates for CoFe-insitu and CoFe LDH. d) Specific activity normalized to ECSA of CoFe-insitu and CoFe LDH catalysts at η =0.3 V.

Table S1. The OER mass activity of CoFe-insitu and benchmarked data of state-of-the-art transition metal-based catalysts in alkaline electrolyte.

Electrocatalysts	Mass acticity	Electrolyte	References
CoFe-insitu	**3.78 A mg^{-1} (η = 0.3 V)**	**1 M KOH**	**This work**

tannin-NiFe complex	9.17 A mg^{-1} (η = 0.3 V)	**1 M KOH**	1
NiFe-based surface-mounted metal–organic frameworks composed of deprotonated terephthalic acid	2.9 A mg^{-1} (η = 0.3 V)	**0.1 M KOH**	2
amorphous NiFeOOH on surface activated carbon fiber paper	2.527 A mg^{-1} (η = 0.27 V)	**1 M KOH**	3
Ni/Co surface-mounted metal–organic framework derivatives	2.5 A mg^{-1} (η = 0.3 V)	**0.1 M KOH**	4
Lattice-strained NiFe MOFs	2 A mg^{-1}_{metal} (η = 0.3 V)	**0.1 M KOH**	5
atomically thin FeCoNi ternary (oxy)hydroxide nanosheets	1.931 A mg^{-1} (η = 0.33 V)	**1 M KOH**	6
amorphous nanocages of Cu-Ni-Fe hydr(oxy)oxide	1.465 A mg^{-1} (η = 0.3 V)	**1 M KOH**	7
Reduced $La_{0.2+2x}Ca_{0.7-2x}Ti_{1-x}Co_xO_3$	1.7 A mg^{-1} (η = 0.45 V)	**1 M KOH**	8
$SrCo_{0.9}Fe_{0.1}O_{3-\delta}$ nanofilms on nickel foam	1000 A g^{-1} (η = 0.55 V)	**1 M KOH**	9
$Sr_2Co_{1.6}Fe_{0.4}O_{4.8}S_{0.2}$	881 A g^{-1} (η = 0.42 V)	**1 M KOH**	10
P–$Ni_{0.75}Fe_{0.25}Se_2$	328.19 A g^{-1} (η = 0.5 V)	**1 M KOH**	11
γ-CoOOH nanosheet	66.6 A g^{-1} (η = 0.3 V)	**1 M KOH**	12

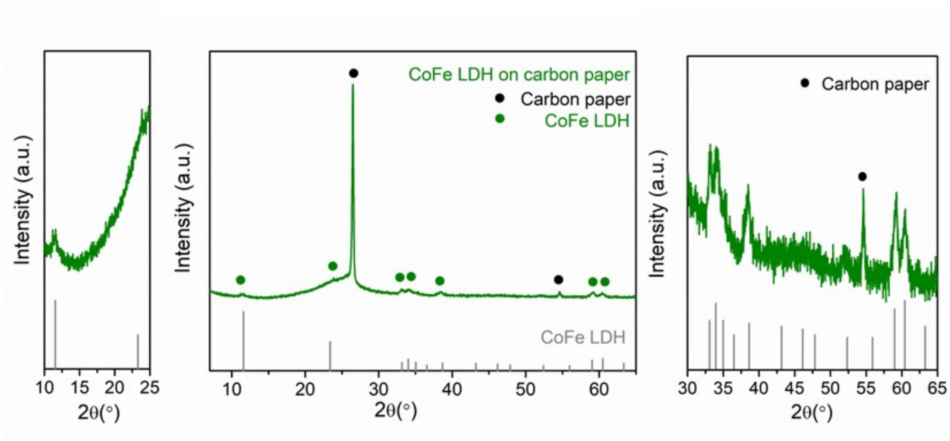

Figure S4. XRD figure of CoFe LDH.

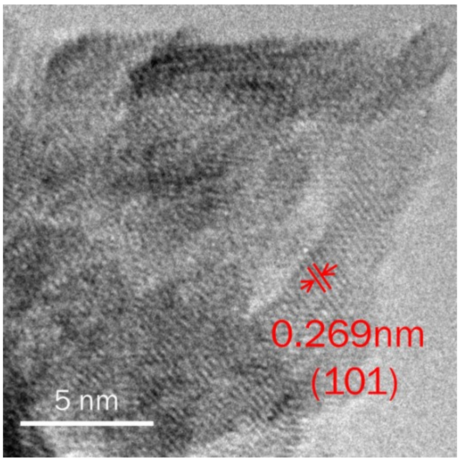

Figure S5. TEM figure of CoFe LDH

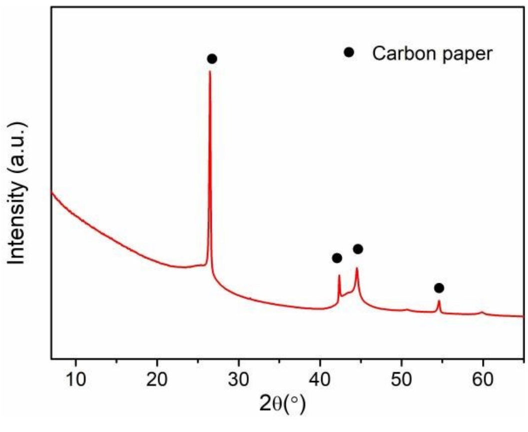

Figure S6. Synchrotron X-ray powder diffraction spectrum of CoFe-insitu

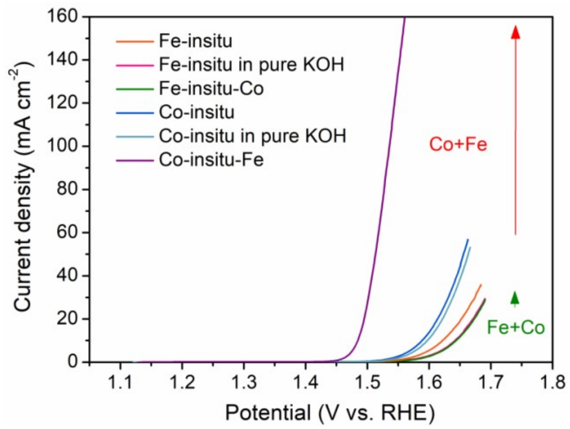

Figure S7. The LSV curves of Co-insitu-Fe and Fe-insitu-Co prepared by two steps in 1 M KOH.

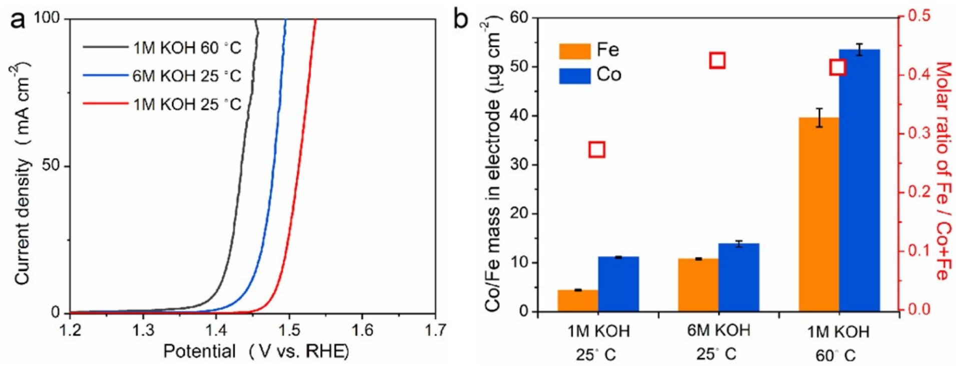

Figure S8 a)The OER polarization curves, b) mass loading of Co and Fe, and molar ratio of Fe/Co+Fe of CoFe-insitu samples synthesized under different KOH concentrations (1M, 6M) and temperatures (25℃, 60℃) .

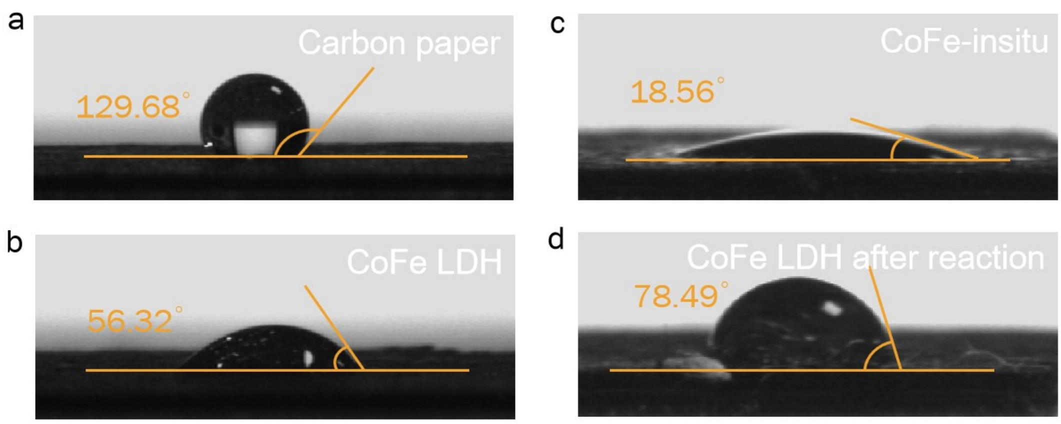

Figure S9. Contact angles of water towards a) blank carbon paper, b) CoFe LDH, c) CoFe-insitu and d) CoFe LDH after OER reaction.

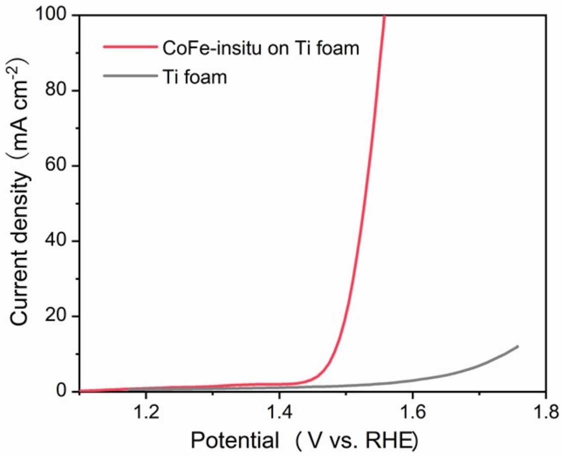

Figure S10. The OER polarization curves of the CoFe-insitu on Ti foam and Ti foam.

Table S2. The elemental concentration on the surface of CoFe-insitu pre and post stability test detect by XPS.

	CoFe-insitu			CoFe-insitu post stability test		
	Atomic conc. [%]	Mass conc. [%]	Fe/Fe+Co	Atomic conc. [%]	Mass conc. [%]	Fe/Fe+Co
O 1s	21.6	24.1	0.456	23.8	23.3	0.472
Fe 2p	1.5	5.7		3.5	12.1	
Co 2p	1.7	7.1		4.0	14.3	
C 1s	75.2	63.1		68.7	50.4	

References

1. Y. Shi, Y. Yu, Y. Liang, Y. Du and B. Zhang, *Angew. Chem. Int. Ed.*, 2019, **58**, 3769-3773.
2. S. Hou, W. Li, S. Watzele, R. M. Kluge, S. Xue, S. Yin, X. Jiang, M. Döblinger, A. Welle, B. Garlyyev, M. Koch, P. Müller-Buschbaum, C. Wöll, A. S. Bandarenka and R. A. Fischer, *Adv. Mater.*, 2021, **33**, 2103218.
3. P. Thangavel, G. Kim and K. S. Kim, *J. Mater. Chem. A*, 2021, **9**, 14043-14051.
4. W. Li, S. Watzele, H. A. El-Sayed, Y. Liang, G. Kieslich, A. S. Bandarenka, K. Rodewald, B. Rieger and R. A. Fischer, *J. Am. Chem. Soc.*, 2019, **141**, 5926-5933.
5. W. Cheng, X. Zhao, H. Su, F. Tang, W. Che, H. Zhang and Q. Liu, *Nature Energy*, 2019, **4**, 115-122.
6. Q. Zhang, N. M. Bedford, J. Pan, X. Lu and R. Amal, *Adv. Energy Mater.*, 2019, **9**, 1901312.
7. Z. Cai, L. Li, Y. Zhang, Z. Yang, J. Yang, Y. Guo and L. Guo, *Angew. Chem. Int. Ed.*, 2019, **58**, 4189-4194.
8. S. Zuo, Y. Liao, C. Wang, A. B. Naden and J. T. S. Irvine, *Small*, 2024, **20**, 2308867.
9. G. Chen, Z. Hu, Y. Zhu, B. Gu, Y. Zhong, H.-J. Lin, C.-T. Chen, W. Zhou and Z. Shao, *Adv. Mater.*, 2018, **30**, 1804333.

10. S. She, Y. Zhu, H. A. Tahini, Z. Hu, S.-C. Weng, X. Wu, Y. Chen, D. Guan, Y. Song, J. Dai, S. C. Smith, H. Wang, W. Zhou and Z. Shao, *Appl. Phys. Rev.*, 2021, **8**, 11407.
11. Y. Huang, L.-W. Jiang, B.-Y. Shi, K. M. Ryan and J.-J. Wang, *Advanced Science*, 2021, **8**, 2101775.
12. J. Huang, J. Chen, T. Yao, J. He, S. Jiang, Z. Sun, Q. Liu, W. Cheng, F. Hu, Y. Jiang, Z. Pan and S. Wei, *Angew. Chem. Int. Ed.*, 2015, **54**, 8722-8727.